Prolate yrast cascade in ^{183}Tl

W. Reviol,[1] M. P. Carpenter,[2] R. V. F. Janssens,[2] D. Jenkins,[3] K. S. Toth,[4] C. R. Bingham,[1,4] L. L. Riedinger,[1]
W. Weintraub,[1] J. A. Cizewski,[2,5] T. Lauritsen,[2] D. Seweryniak,[2] J. Uusitalo,[2] I. Wiedenhöver,[2] R. Wadsworth,[3]
A. N. Wilson,[3] C. J. Gross,[4,6] J. C. Batchelder,[6] K. Helariutta,[7] and S. Juutinen[7]

[1]Department of Physics, University of Tennessee, Knoxville, Tennessee 37996
[2]Physics Division, Argonne National Laboratory, Argonne, Illinois 60439
[3]Department of Physics, University of York, Heslington, York YO1 5DD, United Kingdom
[4]Physics Division, Oak Ridge National Laboratory, Oak Ridge, Tennessee 37831
[5]Department of Physics, Rutgers University, New Brunswick, New Jersey 08903
[6]Oak Ridge Institute for Science and Education, Oak Ridge, Tennessee 37831
[7]Department of Physics, University of Jyväskylä, 40351 Jyväskylä, Finland

The yrast sequence in ^{183}Tl has been studied for the first time in recoil-mass selected γ-ray spectroscopic measurements. A rotational-like cascade of seven transitions is established down to the band head with probable spin and parity $(13/2^+)$. Unlike in the adjacent odd-mass Tl nuclei, prompt γ decay from the yrast band to a lower lying weakly deformed (oblate) structure is not observed. These features are consistent with the predicted drop of the prolate band head in ^{183}Tl compared to ^{185}Tl. The implications for the prolate energy minimum in odd-mass Tl nuclei at the neutron $i_{13/2}$ midshell ($N=103$) are discussed.

PACS number(s): 27.60.+j, 23.20.Lv, 21.60.Cs

I. INTRODUCTION

The mercury-lead region, specifically at $A \lesssim 190$, has provided textbook examples for the shape coexistence phenomenon. Shape transitions from weakly deformed ($\beta_2 \sim 0.15$) oblate (Hg nuclei) or spherical states (Pb nuclei) to excited, well deformed ($\beta_2 \sim 0.25$) prolate minima have been observed at very low spin ($I \gtrsim 2\hbar$) [1–4]. Much of the recent experimental efforts has been devoted to in-beam spectroscopic studies of the neutron deficient Pb isotopes, viz. ^{184,186}Pb, made possible by the use of new, high-efficiency detector systems. In these studies, the prolate minimum at neutron midshell ($N=103$) could be delineated, and compared with that of the Hg isotopes which had been established earlier [5]. The prolate bands in both the even-mass Hg and Pb isotopes are found to minimize in excitation energy at $N=103$ [4,5]. Recent studies of ^{176,178}Hg ($N=96,98$) [6,7] have shown that beyond midshell the prolate minimum rapidly rises with respect to the oblate states. Coexistence between these oblate and prolate shapes is also reported for the light odd-mass Tl nuclei ($Z=81$), see, e.g., Ref. [8]. The low-lying $K^\pi = 9/2^-$ isomeric state in these nuclei, based on the proton $h_{9/2}$ intruder orbital, is the analog to the oblate ground state of the Hg isotopes. Other proton intruder orbitals in the Tl isotopes such as the $i_{13/2}$ states have a low K quantum number on the prolate side and are strongly downsloping as a function of deformation. They are, thus, expected to stabilize the prolate minimum in a way that is analogous to that found in the adjacent Hg and Pb nuclei. Besides the prolate bands built on the $\pi i_{13/2}$ orbital, low-K (prolate) $\pi h_{9/2}$ and $\pi f_{7/2}$ structures have also been observed in ^{187}Tl [9,10] and in ^{185}Tl [10]. However, the prolate yrast band based on the $i_{13/2}$ intruder is predicted [10,11] to continue to drop in excitation energy in the next lighter isotope, ^{183}Tl ($N=102$), in contrast to the midshell behavior of the Hg and Pb isotones which minimize at $N=103$. This trend

presumably reflects the shape-driving nature of the high-j proton intruders involved in the formation of the prolate minimum in the Hg, Tl, and Pb isotopes. Clearly, the exploration of the yrast structure of the Tl isotopes towards lower neutron numbers is of interest.

The results of a study of ^{183}Tl performed with the Gammasphere array [12] at the Argonne Fragment Mass Analyzer (FMA) [13], are discussed in the present paper [14]. This nucleus, as other very neutron-deficient nuclei in this mass region, is difficult to study because the fusion-evaporation cross sections are small compared to a fission yield that accounts for >95% of the decay of the compound system. Hence, in order to achieve the required detection sensitivity, in-beam γ-ray spectroscopic methods need to be combined with mass separation of the recoiling nuclei and, if possible, with recoil (α- or proton-) decay tagging (RDT) [15]. However, the α-decay branch of the 60 ms, $9/2^-$ isomer in ^{183}Tl has recently been measured to be only ~1.5% [16]. This makes the RDT technique less suitable and the results presented hereafter are mainly based on spectroscopy following mass identification, where the isotopic identification relies on the observation of the characteristic x rays.

II. EXPERIMENT AND RESULTS

States in ^{183}Tl were populated using the ^{108}Pd(^{78}Kr,$p2n$) reaction at 340 MeV with a 0.83 mg/cm^2 self-supporting target enriched to >98% in ^{108}Pd. The target was located at the center of the Gammasphere array, which contained at the time of the experiment 97 large-volume Ge detectors, all surrounded by BGO Compton suppressor shields, and four planar Ge counters (LEPS). The prompt γ radiation emitted from the target was observed for as long as the recoils remained in the line of sight of the Ge detectors, i.e., during a time range of about 30 ns after the reaction occurred. These γ rays were detected in coincidence with the information provided by the mass analysis from the FMA. This instru-
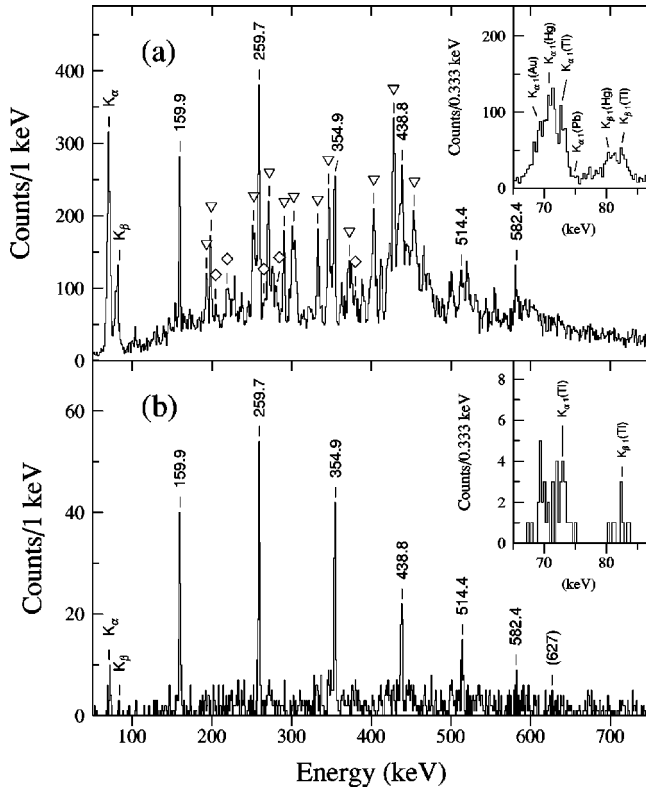
FIG. 1. Spectra of prompt γ rays from the target in coincidence with $A=183$ events in the focal plane x-y position spectrum. (a) Total projection; known transitions in ^{183}Hg and ^{183}Au are labeled by triangles and diamonds, respectively. Newly observed transitions are labelled by their energies in keV. The inset shows the x-ray region at a larger dispersion of 1/3 keV per channel. (b) Sum of projections from the $A=183$ selected E_γ-E_γ coincidence data with gates on the 159.9-, 259.7-, 354.9-, 438.8-, and 514.4-keV lines. The inset shows the x-ray region of the spectrum (1/3 keV per channel) gated by the three lowest-energy lines.

ment was set up so that the central trajectories corresponded to mass $A=183$ and 184 ions with charge states $Q=30,31,32$. The time-of-flight (TOF) of the recoils from the target to the FMA focal plane was determined to be ~720 ns. At the focal plane, the A/Q ratio of the evaporation residues was determined from a position measurement using a parallel-grid avalanche counter (PGAC). The nuclei were subsequently implanted in a double-sided Si strip detector (DSSD, 1600 1×1 mm pixels) located 40 cm downstream. The energies of recoils (E_r) and of the decay particles (E_α) as well as the associated positions were measured together with the time stamp of the event. In addition, the TOF of the recoils from the PGAC to the DSSD was also measured. A total of $\sim10^8$ events were recorded, corresponding either to recoil-γ^n ($n\geqslant1$) or to any event detected in the DSSD (implants or particle decays). The position spectrum at the focal plane of the FMA was dominated by events associated with $A=183$ nuclei. Mass $A=184$ residues had more than two times less yield while $A=180$, 181, and 182 recoils were roughly five times weaker.

In Fig. 1(a), the γ-ray spectrum gated on $A=183$ is shown. This spectrum was obtained by requiring that the

appropriate PGAC x and y positions and that the TOF conditions between Gammasphere and PGAC and between PGAC and DSSD be satisfied. The bump between 400 and 500 keV in Fig. 1(a) is a remnant of the very strong Coulomb excitation peaks from both the projectile and the target nuclei. Most of the strong γ-ray lines in the spectrum can be readily identified as known transitions in ^{183}Hg [17] and ^{183}Au [18]. The remaining strong peaks labeled by their energies (in keV) in Fig. 1(a) are newly observed. These peaks with respective energies of 159.9, 259.7, 354.9, 438.8, 514.4, and 582.4 keV were established to be in coincidence with each other, as inferred from a mass-gated E_γ-E_γ matrix which included γ-ray double and unpacked triple and higher fold events. Fig. 1(b) presents the sum of coincidence spectra gated on all of the new γ-ray lines between 159.9 and 514.4 keV. The new sequence of γ rays is assigned to the nucleus ^{183}Tl, based on the absence of coincidence relationships with the known transitions in ^{183}Hg or ^{183}Au, and on the presence of coincident Tl x rays. The gated x-ray spectrum is displayed with a larger dispersion in the inset of Fig. 1(b). It clearly shows an enhancement of the Tl K_α line when compared to the corresponding "total" $A=183$ spectrum [inset of Fig. 1(a)]. Interestingly, a detailed analysis of the $A=183$ γ-ray spectrum shows that ^{183}Tl, the final nucleus produced in the $p2n$ evaporation channel, is weaker than the $2pn$ channel leading to ^{183}Hg, but stronger than the $3p$ channel leading to ^{183}Au. This observation is in qualitative agreement with statistical model calculations using the program EVAPOR [19] and is, thus, consistent with the proposed isotopic assignment.

The main features of the spectrum in Fig. 1(b) are (i) the regular energy spacings of the peaks, (ii) the absence of additional peaks that would alter this spacing, and (iii) an intensity pattern consistent with the placement of these γ rays in a regular, rotational-like cascade with increasing transition energies. Clearly, this spectrum displays the yrast sequence of ^{183}Tl, and its rotational behavior resembles closely that exhibited by the yrast sequences of the neighboring, heavier odd-mass Tl isotopes. It is, however, striking that no additional excited states in ^{183}Tl were observed from the mass-gated γ-ray coincidence matrix.

As a complementary approach to identify new states in ^{183}Tl, an RDT analysis was also performed for the present data set. The results of this analysis are presented in Fig. 2. The top histogram is the spectrum obtained by requiring that the recoil-γ event be in coincidence with a subsequent ^{183}Tl α decay ($E_\alpha=6.40$ MeV) occurring in the same DSSD pixel as the implant within a time interval $\Delta t=180$ ms (corresponding to three ^{183}Tl α decay half-lives [20]). The bottom γ-ray spectrum in Fig. 2 is obtained by requiring instead a coincidence with the ground state α decay of ^{180}Hg [17] ($E_\alpha=6.12$ MeV, $\Delta t=8.4$ s). This nucleus is populated via the $\alpha2n$ evaporation channel. In this case, the $E_\alpha=6.12$ MeV line represents a rather large α branch ($b_\alpha=48\%$), and the α-γ correlation spectrum can be viewed as a demonstration of the effectiveness of the RDT technique under the present experimental conditions [21]. Indeed, the known yrast transitions in ^{180}Hg [5] can be readily identified. Focusing on the top RDT γ-ray spectrum, it is obvious that the
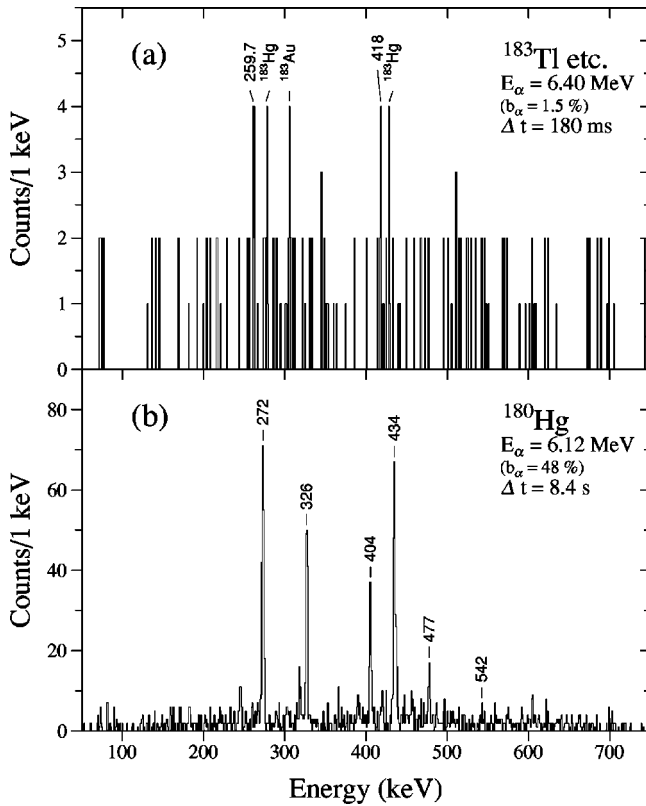
FIG. 2. Energy spectra of γ rays generated by using the RDT technique. (a) The γ rays correlated with the ^{183}Tl α decay, see text. (b) Spectrum of γ rays tagged by the ground state α decay of ^{180}Hg from the same experiment.

FIG. 3. Proposed level scheme for ^{183}Tl. The uncertainties for the γ-ray transition energies range from 0.2 to 1 keV. The widths of the filled and open arrows represent the γ-ray and internal conversion intensities, respectively. The latter are calculated for the indicated transition multipolarities. The assignment of spins and positive parity to the yrast band is based on analogies with structures in neighboring Tl isotopes. Note that a link between the yrast band and the lower energy levels was not observed. An upper limit for the energy of the $(13/2^+)$ state is given in the text. The energies of the $3/2^+$ and $9/2^-$ levels and the quoted half-life are adopted from independent α-decay work (Refs. [16,20]).

small α branch ($b_\alpha \sim 1.5\%$) results in a lack of statistics and, hence, this spectrum cannot provide significant new information on levels in ^{183}Tl. A careful search in the mass-gated γ-ray data for possible coincidence relationships between the peaks in Fig. 2(a) and the yrast transitions in ^{183}Tl proved inconclusive. Instead, with the exception of a 418-keV γ-ray, the peaks weakly seen in the spectrum of Fig. 2(a) were found to correspond to strong peaks in the $A=183$ γ-ray spectrum and are most likely random contributions to the coincidence spectrum gated by the ^{183}Tl$^m \alpha$ particles. The weak 418-keV γ ray is possibly a transition in ^{183}Tl, however, it cannot be assigned with confidence to this nucleus.

III. LEVEL SCHEME

The proposed level scheme for ^{183}Tl is shown in Fig. 3. The low-lying levels up to the $9/2^-$ isomeric state have been established in independent α-decay work [16]; all higher-lying states are observed in the present work. The 627-keV transition should be considered as tentative and is marked accordingly. Unfortunately, the present data do not allow the determination of γ-ray anisotropies for the transitions of interest. Therefore, spins and parities of the levels above the $9/2^-$ state are assigned by comparison with the yrast sequences in neighboring odd-mass Tl nuclei. On the basis of intensity considerations, the 159.9-keV γ ray is identified as an $E2$ transition and placed at the bottom of the band. Figure
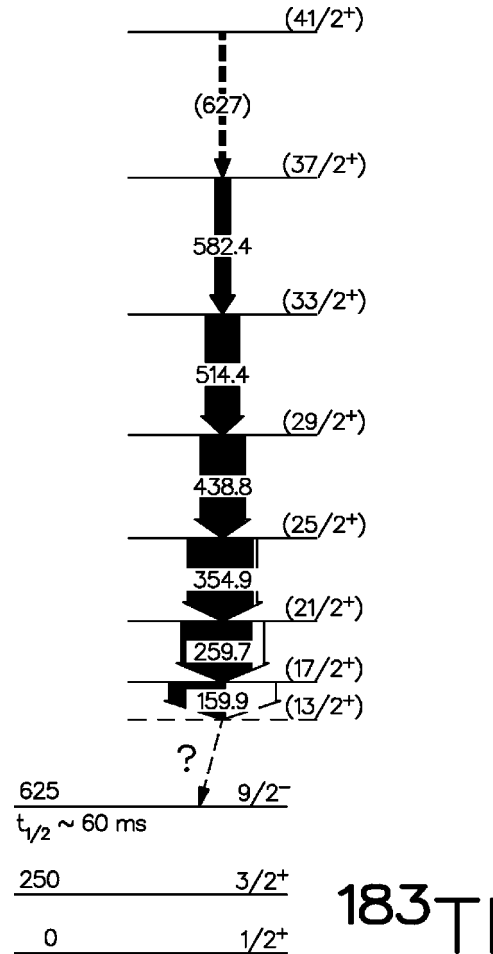
4 shows the intensity pattern of the ^{183}Tl band, after correction for detection efficiency and internal conversion, with that of the yrast $\pi i_{13/2}$ band in the nearest neighboring isotope ^{185}Tl [10] (the intensity patterns of the same bands in the heavier isotopes are also very similar). An $E2$ assignment for the strongly converted 159.9-keV γ ray in ^{183}Tl ensures intensity conservation over the entire cascade, while an $M1$ assignment is clearly ruled out. An $E1$ assignment would imply a deviation from the usual side feeding of yrast states (e.g., in ^{185}Tl) and is deemed unlikely.

As indicated in Fig. 3, it appears that the $\pi i_{13/2}$ band in ^{183}Tl is populated all the way down to the $(13/2^+)$ band head. This feature is different from the bottom part of the yrast structures in the two neighboring odd-mass isotopes ^{185,187}Tl. There, the $17/2^+ \rightarrow 13/2^+$ transition can be viewed as a "decay-out" transition, i.e., the $13/2^+$ level observed
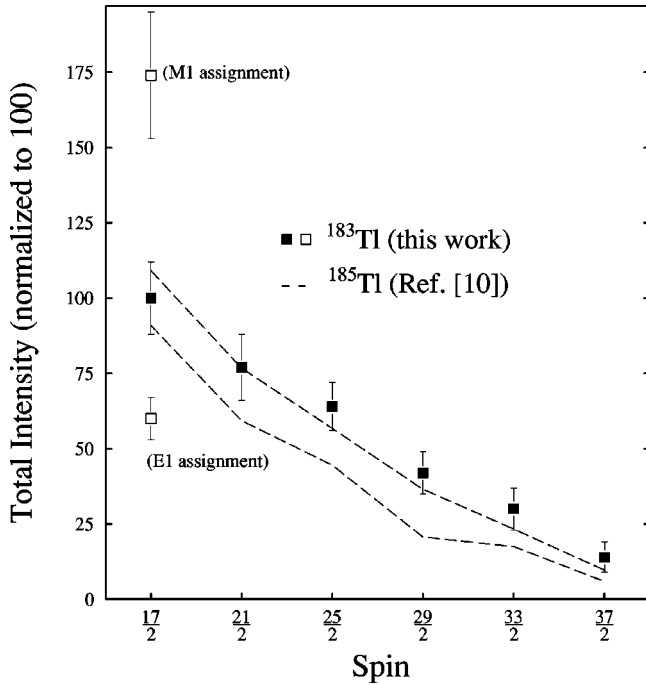
FIG. 4. Total intensity as a function of initial spin for the yrast bands in ^{183}Tl and ^{185}Tl. The area shown for ^{185}Tl represents the conversion-corrected intensity with error. A common normalization is used to ease the comparison of these intensity patterns.
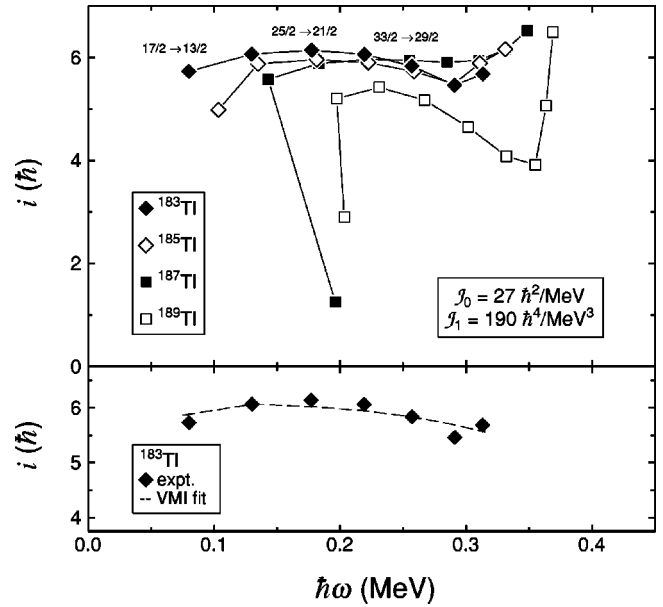

FIG. 5. Aligned angular momenta for the positive-parity yrast bands in odd-*A* Tl isotopes using a rotating reference described by $\mathcal{J}_0 = 27\ \hbar^2/\text{MeV}$ and $\mathcal{J}_1 = 190\ \hbar^4/\text{MeV}^3$. The corresponding spins are indicated for every other $E2$ transition. Bottom: Comparison for ^{183}Tl between experimentally obtained *i* versus $\hbar\omega$ data and calculated values based on a VMI fit (see text for details).

does not belong to the prolate band structure but is assigned instead to another intrinsic excitation. In ^{185,187}Tl, this $13/2^+$ level then feeds via an $E1$ transition into a lower-lying level structure based on the oblate $9/2^-$ isomeric state. As already mentioned, there is no evidence for γ rays of significant strength in ^{183}Tl other than the transitions of the yrast band. Specifically, in the spectral ranges between 100 and 150 keV and 400 and 500 keV additional transitions (belonging to an oblate level structure) would be expected if the location of the yrast band in ^{183}Tl relative to the low-lying $9/2^-$ state was similar to that seen in ^{185}Tl (see Ref. [10], Fig. 8), but not a single γ ray is observed. A γ decay from the $(13/2^+)$ band head to the $9/2^-$ isomeric state is not observed in the present data either. This observation suggests that the half-life of the crucial $M2$ transition is rather long — i.e., not in the sensitive range for detection of γ radiation from the target ($\sim$30 ns). It also has implications for the excitation energy of the yrast band relative to the $9/2^-$ state, as discussed in Sec. IV.

IV. DISCUSSION

In Fig. 5 (top), the aligned angular momentum *i* as a function of rotational frequency $\hbar\omega$ is presented for the yrast sequences with spin $I^\pi \geq 13/2^+$ in ^{183}Tl, ^{185,187}Tl [10], and ^{189}Tl [8,22]. The same Harris parametrization $\mathcal{J}_0 = 27\hbar^2/\text{MeV}$ and $\mathcal{J}_1 = 190\hbar^4/\text{MeV}^3$, was used for the extraction of *i* in the four isotopes. In the case of ^{189}Tl, a $17/2^+ \rightarrow 13/2^+$ transition is omitted in Fig. 5 because of a shape change along the yrast line around $17/2\ \hbar$, two angular momentum units higher than in the lighter isotopes. The

alignment of $\sim 6\hbar$ observed in the flat part of the *i* vs $\hbar\omega$ curves (0.15 MeV $\leq\hbar\omega\leq$0.3 MeV, $17/2\leq I\leq37/2$) is expected for a rotation aligned proton and the measured values support an $i_{13/2}[660]1/2$ configuration assignment. At $\hbar\omega\sim$0.35 MeV, there is evidence for a rotational alignment in all these nuclei. The latter is of $(\nu i_{13/2})^2$ character, as shown in Ref. [22]. It is worth noting that in the flat range of the alignment curves the yrast bands of the four isotopes display the trend of an increase in alignment with decreasing neutron number. This systematic feature is indicative of a gradual increase in rotational behavior with decreasing mass, where ^{183}Tl represents the best example to date for a well-deformed prolate rotor in the isotopic chain of Tl nuclei. In this context, the trend with mass exhibited by the $17/2^+ \rightarrow 13/2^+$ transitions in ^{183,185,187}Tl also deserves attention. While this transition appears to be part of the rotational sequence in ^{183}Tl, it deviates considerably in ^{185,187}Tl (Fig. 5), and can be understood as the link between the yrast band and another, lower-lying positive-parity structure [10] (see description given in Sec. III above). The placement of the 159.9-keV transition in ^{183}Tl as an inband transition is supported by a variable moment of inertia (VMI) fit [23] to the yrast energy levels between $(17/2^+)$ and $(37/2^+)$. The values of the achieved fitting parameters $\mathcal{J}_0 = 2.78\ 10^{-2}$ keV^{-1} and $C = 2.98\ 10^6$ keV^3, are close to those reported for ^{185,187}Tl [10] (a precise knowledge of the $E(13/2^+)$ band-head energy is not necessary for this purpose). The $i(\hbar\omega)$ values resulting from the VMI fit are compared with the experimental values in the bottom part of Fig. 5: experimental and calculated alignments are in reasonable agreement, thus qualifying the measured $(17/2^+)\rightarrow(13/2^+)$ transition in ^{183}Tl as an unperturbed member of the $\pi i_{13/2}$

TABLE I. Upper limit estimate for the $(13/2^+)$ to $9/2^-$ energy difference E_{rel} in ^{183}Tl, based on lifetime considerations (see text).

E_{rel}	$t_{1/2}(M2)$ [a]	$\Delta E(13/2^+ \rightarrow 11/2^-)$ [b]	$t_{1/2}(E1)$ [a]	$\Delta E(11/2^- \rightarrow 9/2^-)$ [d]	$t_{1/2}(M1)$ [a]
500 keV	30 ns [b]	2 keV	27 ns	498 keV	0.2 ps
		8 keV [c]	300 ps	492 keV	0.2 ps
		90 keV [c]	0.3 ps	410 keV	0.3 ps

[a]Half-lives according to a Weisskopf estimate.
[b]Assumed $(13/2^+) \rightarrow 11/2^-$ energy difference ($E1$ transition).
[c]Hindrance factor $HF \sim 10^2$ considered for the $E1$ transition according to Ref. [24].
[d]Energy difference E_{rel}-$\Delta E(13/2^+ \rightarrow 11/2^-)$ corresponding to the following $M1$ transition.

band. By the same token, the band head of this $\pi i_{13/2}$ sequence is the lowest $13/2^+$ state in ^{183}Tl.

Since the decay of the $(13/2^+)$ state could not be established in the present experiment, it is pertinent to discuss possible scenarios for the decay out of the $\pi i_{13/2}$ band in ^{183}Tl. The goal of this discussion is to derive a realistic estimate for the upper limit of the excitation energy E_{rel} of the $(13/2^+)$ band head with respect to the $9/2^-$ isomeric state. The absence of a perturbation in energy for the location of the $(13/2^+)$ level limits possible scenarios to two cases, (i) an $(13/2^+) \rightarrow 9/2^-$ $M2$ transition $[E_\gamma(M2)=E_{rel}]$ and (ii) a decay to the $9/2^-$ state in two steps starting with an $(13/2^+) \rightarrow (11/2^-)$ $E1$ transition. The assumptions that can be made for both cases are summarized in Table I. From the aforementioned time constraints for detection of γ radiation from the target, a lower limit of 30 ns for the half-life of the $(13/2^+)$ level is obtained. This corresponds to an upper limit $E_{rel}=500$ keV, according to a Weisskopf estimate, where the γ-ray strength for the $M2$ transition is assumed to be unhindered [a hindrance factor $HF(M2)=1$ is recommended for $A>150$ nuclei [24]]. It can be shown that $E_{rel} \lesssim 500$ keV is a conservative estimate for the $(13/2^+)$ level by investigating the competition between possible $(13/2^+) \rightarrow 9/2^-$ $M2$ and $(13/2^+) \rightarrow 11/2^-$ $E1$ transitions. As indicated in Table I, the $E1$ and $M2$ decay strengths would be comparable if $E_\gamma(E1) \lesssim 2$ keV or, very similar, if $E_\gamma(E1) \lesssim 8$ keV $[HF(E1) \sim 10^2$ for $A>150$ [24]]. In this scenario, the $E1$ transition would not be observed but a coincidence relationship between the subsequent $11/2^- \rightarrow 9/2^-$ $M1$ transition and the members of the $\pi i_{13/2}$ yrast band would be likely. However, this $M1$ transition would have an energy of ~ 500 keV and would break the trend of $11/2^- \rightarrow 9/2^-$ transitions (oblate) as a function of N seen in the neighboring Tl isotopes. In the isotopic chain from ^{189}Tl to ^{185}Tl, the $M1$ transition energies under discussion systematically increase by about 10 keV from one isotope to the next lighter one [8–10] and a corresponding transition in ^{183}Tl would be expected to have an energy of about 410 keV, which is inconsistent with the present scenario. On the other hand, if an $E1$ transition with a significantly larger energy than assumed above was present, e.g., with ~ 90 keV (and thus matching with a subsequent ~ 410 keV $M1$ transition), the decay strength would be focused in this sequence, similar to the situation in the neighboring Tl isotopes. However, such an $E1$-$M1$ sequence is not observed in ^{183}Tl, as already empha-

sized in the previous section. Therefore, a decay of the $(13/2^+)$ state via an $E1$ transition is ruled out and an $(13/2^+) \rightarrow 9/2^-$ $M2$ transition seems to be the most likely decay path. To proceed, a conservative upper limit $E_{rel}=500$ keV for the $(13/2^+)$ state is then assumed in the remaining discussion below.

Figure 6 compares experimentally obtained prolate to oblate energy differences for the near-yrast coexisting level structures in odd Tl isotopes. These data are given relative to the oblate $9/2^-$ isomeric state (labeled with [505] asymptotic quantum numbers and taken from Ref. [17]). The prolate bandheads for $^{185-189}$Tl represent extrapolated values based on VMI fits of the $i_{13/2}$ sequences [10]. For ^{183}Tl ($N=102$),
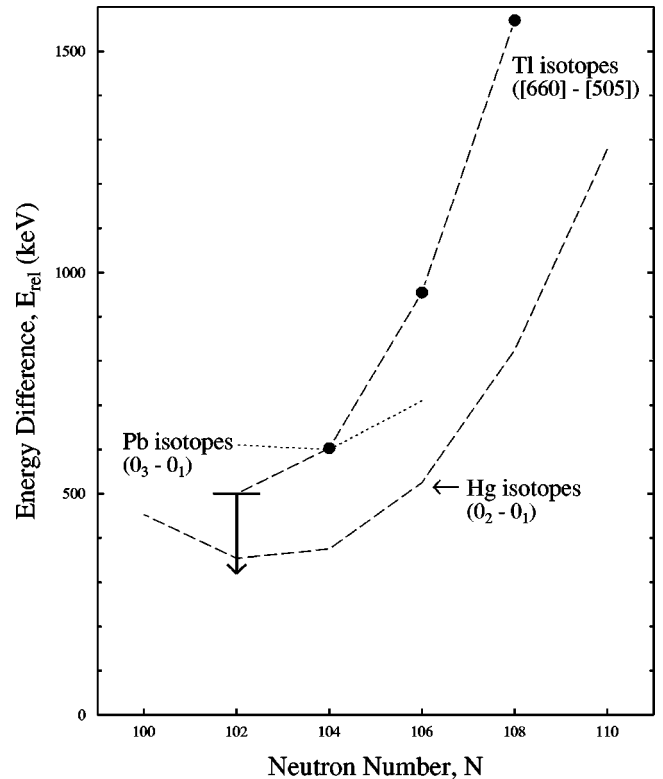

FIG. 6. Excitation energy of the prolate $i_{13/2}$ level structures in the Tl isotopes relative to the corresponding [505]$9/2^-$ isomeric states as a function of neutron number. The data point for ^{183}Tl ($N=102$) represents an upper limit, as discussed in the text. The prolate to oblate and prolate to spherical energy differences in the Hg and Pb isotopes are also given for comparison.

the new information obtained from the above upper limit on $E_{\rm rel}$ is displayed. Also included in Fig. 6 are the energy differences between prolate band heads (extrapolated 0_2^+ states [1,5]) and the oblate ground state in the Hg isotones and, likewise, relative energies for the Pb nuclei (extrapolated 0_3^+ minus 0_1^+ [4]). As stated above, the oblate states in Hg and Tl nuclei are understood as corresponding to similar (weak) deformations and, thus, represent a common "reference" in the present comparison. The $E_{\rm rel}$ values for the Pb isotopes correspond to a prolate to spherical energy difference, but are quite comparable with the systematics shown for the Tl and Hg isotopes since the differences in deformation are similar.

The prolate to oblate energy differences in Tl nuclei as a function of neutron number follow approximately the trend seen in the corresponding Hg isotones for $N \geq 104$ (dashed lines). However, near $N = 103$ (neutron $i_{13/2}$ midshell) the prolate band in Hg nuclei reaches its minimum energy, while the corresponding band in the Tl nuclei continues its downsloping trend with decreasing N. According to Fig. 6, $E_{\rm rel}$ changes by at least 100 keV between $N = 104$ and 102. For the even-mass Pb isotopes the prolate to spherical energy differences minimize again near $N = 103$, as in the Hg isotopic chain, as already emphasized in Ref. [4]. On the other hand, the $\pi i_{13/2}$ prolate intruder bands in the neighboring Au isotopes, ^{179}Au [25] and ^{181,183}Au [18] (not shown in Fig. 6), are recognized to minimize in excitation energy even at $N < 100$ — i.e., they behave in a way similar to the yrast bands in the Tl isotopes. Mean field calculations for these Tl and Au isotopes, presented in Refs. [10], [11], and [18] respectively, predict that the prolate yrast states in odd-mass Tl nuclei continue to drop in excitation energy past midshell, in agreement with the present results. These findings indicate that the odd proton has considerable impact on the formation of the prolate minimum and it is possible that the $i_{13/2}$ proton polarizes the core. However, as stated in Ref. [10], further theoretical investigations are necessary to better understand the difference in the midshell behavior between the Tl isotopes and the even-Z neighboring nuclei.

V. CONCLUSIONS

The yrast sequence in ^{183}Tl has been observed for the first time in recoil-mass selected γ-ray spectroscopic measurements. The new sequence resembles the well-deformed (prolate) excited bands in adjacent Hg, Tl, and Pb nuclei, but its decay-out properties are different from those other cases in two respects. (i) The rotational-like sequence is observed from medium spin down to the band head. (ii) A strong, prompt γ decay from the prolate band to a less deformed, lower-lying structure is not observed. The excitation energy of the $(13/2^+)$ band head is not precisely known. Nevertheless, based on lifetime considerations a conservative upper limit estimate for $E(13/2^+)$ is obtained that provides circumstantial evidence for a considerable drop in excitation energy of the prolate yrast states in ^{183}Tl compared to ^{185}Tl. This estimate implies also that the decay of the $(13/2^+)$ band head proceeds by a rather low-energy $M2$ γ ray to the oblate $9/2^-$ isomeric state (probably associated with a half-life that is significantly larger than 30 ns). The experimental observations are consistent with theoretical calculations predicting that the prolate energy minimum in the Tl nuclei continues to drop past midshell ($N \sim 103$), in contrast to the neighboring Hg and Pb isotopes where the prolate states are predicted and observed to minimize at midshell. Clearly, a new experiment with a higher detection sensitivity for the decay out of the yrast sequence would be desirable to resolve the shortcomings of the present level scheme.

[1] J.L. Wood, K. Heyde, W. Nazarewicz, M. Huyse, and P. Van Duppen, Phys. Rep. **215**, 211 (1992), and references therein.

[2] J. Heese, K.H. Maier, H. Grawe, J. Grebosz, H. Kluge, W. Meczynski, M. Schramm, R. Schubart, K. Spohr, and J. Styczen, Phys. Lett. B **302**, 390 (1993).

[3] A.M. Baxter *et al.*, Phys. Rev. C **48**, R2140 (1993).

[4] J.F.C. Cocks *et al.*, Eur. Phys. J. A **3**, 17 (1998).

[5] G.D. Dracoulis, A.E. Stuchbery, A.O. Macchiavelli, C.W. Beausang, J. Burde, M.A. Deleplanque, R.M. Diamond, and F.S. Stephens, Phys. Lett. B **208**, 365 (1988).

[6] M.P. Carpenter *et al.*, Phys. Rev. Lett. **78**, 3650 (1997).

[7] M. Muikku *et al.*, Phys. Rev. C **58**, R3033 (1998).

[8] M.G. Porquet *et al.*, Phys. Rev. C **44**, 2445 (1991).

[9] W. Reviol *et al.*, Phys. Rev. C **49**, R587 (1994).

[10] G.J. Lane, G.D. Dracoulis, A.P. Byrne, P.M. Walker, A.M. Baxter, J.A. Sheikh, and W. Nazarewicz, Nucl. Phys. **A586**, 316 (1995).

[11] K. Heyde, M. Waroquier, H. Vincx, and P. Van Isacker, Phys. Lett. **64B**, 135 (1976); (private communication).

[12] I.Y. Lee, Nucl. Phys. **A520**, 641c (1990).

[13] C.N. Davids, B.B. Back, K. Bindra, D.J. Henderson, W. Kutschera, T. Lauritsen, Y. Nagame, P. Sugathan, A.V. Ramayya, and W.B. Walters, Nucl. Instrum. Methods Phys. Res. B **70**, 358 (1992).

[14] An early account of this study has been reported by W. Reviol *et al.*, in the *Proccedings of the Conference "Nuclear Structure 98,"* Gatlinburg, Tennessee, 1998, AIP Conf. Proc. No. 481 (AIP, New York, 1999), p. 232.

[15] E.S. Paul *et al.*, Phys. Rev. C **51**, 78 (1995).

[16] J.C. Batchelder *et al.*, Eur. Phys. J. A **5**, 49 (1999).

[17] E.S. Firestone and V.S. Shirley, *Table of Isotopes*, 8th ed. (Wiley, New York, 1996), Vol. II

[18] W.F. Mueller *et al.*, Phys. Rev. C **59**, 2009 (1999).

[19] J.R. Beene and N.G. Nicolis, computer code EVAPOR (unpub-

lished); evolved from the code PACE by A. Gavron, Phys. Rev. C **21**, 230 (1980).

[20] U.J. Schrewe *et al.*, Phys. Lett. **91B**, 46 (1980).

[21] A detailed analysis of the α spectra measured in the course of this experiment will be presented in a separate paper by A.N. Wilson.

[22] W. Reviol *et al.* (unpublished).

[23] The band energies have been fitted using an expression $E_I = E(13/2^+) + 1/2C(\mathcal{J}_I - \mathcal{J}_0)^2 + R(R+1)/2\mathcal{J}_I$ with $R = \sqrt{(I+1/2)^2 - K^2} - i - 1/2$, $K = 1/2$, and $i = 6$ (cf. Fig. 5). This is consistent with the expression introduced by M.A. Mariscotti, G. Scharff-Goldhaber, and B. Buck, Phys. Rev. **178**, 1864 (1969).

[24] J.K. Tuli, Nucl. Data Sheets **86**, 9 (1999).

[25] W.F. Mueller *et al.*, in University of Tennessee progress report, 1997 (unpublished); W.F. Mueller *et al.* (unpublished).